

Accepted Manuscript

Optimization of layered regenerator of a magnetic refrigeration device

Behzad Monfared, Björn Palm

PII: S0140-7007(15)00126-7

DOI: [10.1016/j.ijrefrig.2015.04.019](https://doi.org/10.1016/j.ijrefrig.2015.04.019)

Reference: JIJR 3034

To appear in: *International Journal of Refrigeration*

Received Date: 10 March 2015

Revised Date: 15 April 2015

Accepted Date: 26 April 2015

Please cite this article as: Monfared, B., Palm, B., Optimization of layered regenerator of a magnetic refrigeration device, *International Journal of Refrigeration* (2015), doi: 10.1016/j.ijrefrig.2015.04.019.

This is a PDF file of an unedited manuscript that has been accepted for publication. As a service to our customers we are providing this early version of the manuscript. The manuscript will undergo copyediting, typesetting, and review of the resulting proof before it is published in its final form. Please note that during the production process errors may be discovered which could affect the content, and all legal disclaimers that apply to the journal pertain.



Optimization of layered regenerator of a magnetic refrigeration device

Behzad Monfared^{a,*}, Björn Palm^a

^a KTH Royal Institute of Technology, School of Industrial Engineering and Management, Department of Energy Technology, Brinellvägen 68, SE-100 44 Stockholm, Sweden

* Corresponding author. Tel.: +46 8 790 81 54; fax.: +46 8 20 41 61.

E-mail address: behzadam@kth.se (Behzad Monfared)

Abstract

Magnetic refrigeration, as an alternative to vapor-compression technology, has been the subject of many recent investigations. A technique to enhance the performance of magnetic refrigerators is using layers of different materials in the regenerator of such devices. In this study the choice of magnetocaloric materials in a multi-layered packed bed regenerator is investigated in order to optimize the performance. A numerical model has been developed to simulate the packed bed in this study. Optimized packed bed designs to get maximum temperature span or maximum efficiency are different. The results indicate that maximum temperature span can be achieved by choosing the materials with the highest magnetocaloric effect in the working temperature range, while maximum Carnot efficiency is achieved by choosing materials with Curie temperatures above the average layer temperature.

Keywords: magnetic refrigeration, magnetocaloric, layering, optimization, temperature span, efficiency

Nomenclature:

a	specific surface area, ratio of heat transfer surface area of particles to volume of bed [m^{-1}]
$A_{c,bed}$	cross section area of a bed [m^2]
B	magnetic field [T]
Co	cobalt
c_H	constant-field specific heat capacity [$\text{Jkg}^{-1}\text{K}^{-1}$]
c_p	constant-pressure specific heat capacity [$\text{Jkg}^{-1}\text{K}^{-1}$]
D	diameter of packed bed [m]

d_p	diameter of particles [m]
Dy	dysprosium
Er	erbium
Fe	iron
Gd	gadolinium
Ge	germanium
h	convection heat transfer coefficient in regenerator [$\text{Wm}^{-2}\text{K}^{-1}$]
i	enthalpy [Jkg^{-1}]
k	thermal conductivity [$\text{Wm}^{-1}\text{K}^{-1}$]
La	lanthanum
\dot{m}	mass flow rate [kgs^{-1}]
Nd	neodymium
Ni	nickel
P	pressure [Pa]
Pd	palladium
Pr	Prandtl number [-]
Q_C	cooling capacity [W]
Q_H	heating capacity [W]
Re_d	Reynolds number, $\rho_f V_D \cdot d_p / \mu_f$ [-]
s	entropy [$\text{Jkg}^{-1}\text{K}^{-1}$]
Si	silicon
T	temperature [K]
t	time [s]
Tb	terbium
U	overall heat transfer coefficient for ambient-bed heat transfer [$\text{Wm}^{-2}\text{K}^{-1}$]

V_D volumetric flow rate divided by cross section area of regenerator [ms^{-1}]

x position along regenerator [m]

Greek symbols

Δs_M magnetic entropy change [$\text{Jkg}^{-1}\text{K}^{-1}$]

ε porosity [-]

η_{Carnot} Carnot efficiency [-]

μ viscosity [Pas]

ρ density [kgm^{-3}]

τ cycle period [s]

Subscripts

amb ambient

C cold reservoir

e effective

f heat transfer fluid

H hot reservoir

L fluid leaving the regenerator

R fluid returning from heat exchanger

s solid phase in regenerator

sf solid-fluid interface in regenerator

1 Introduction

In recent years magnetic refrigeration at room temperature, as an alternative to the vapor-compression technology, has been the subject of many research works. The motivation behind the research in this field is, mainly, to reach higher efficiencies and less environmental impacts compared to vapor-compression technology. Monfared et al. (2014) have shown through life cycle assessment (LCA) that if a magnetic refrigerator operates more efficiently than a vapor-compression refrigerator it can be less harmful to the environment in some aspects.

One of the solutions to improve the performance of a magnetic refrigerator is to have layers of different materials in the packed beds instead of only one specific material. While a magnetic refrigerator is operating, a temperature span is established between the two ends of the bed, which means that the temperatures at different positions along the bed are different at each moment of a cycle. Considering the fact that the magnetocaloric materials show higher magnetocaloric effect about their transition temperature, materials with different transition temperatures can be used along the bed to enhance the performance.

Among investigations on second order phase transition materials for room temperature applications with tunable transient temperature, the works of Canepa et al. (2002) and Dai et al. (2000) who worked on $Gd_7Pd_{3-x}Ni_x$ and $(Gd,Dy)_{1-x}Nd_x$ alloys can be mentioned. By changing the composition of $Gd_7Pd_{3-x}Ni_x$ and $(Gd,Dy)_{1-x}Nd_x$ alloys, different transition temperatures, both higher and lower than that of Gadolinium, can be obtained. After discovery of the so-called giant magnetocaloric effect in $Gd_5Si_2Ge_2$ in 1997, $Gd_5(Si_{1-x}Ge_x)_4$ materials, the transition temperature of which can be varied through changing Si:Ge ratio, have been investigated (Pecharsky et al., 2002). Among newer materials different compositions of $MnFe(P,Si,Ge)$ can also be used for layering the regenerator of a magnetic refrigerator. $MnFe(P,Si,Ge)$ compounds have high magnetic entropy change and no rare-earth elements (Cam Thanh et al., 2007).

Richard et al. (2004) showed that a two-layered bed consisting of Gd and $Gd_{0.74}Tb_{0.26}$ (with equal length of layers) can produce larger temperature span at no-load condition and can give higher cooling capacity at larger spans compared to a single-layered bed of Gd. Later Rowe and Tura (2006) used three layers of equal length of the materials Gd, $Gd_{0.74}Tb_{0.26}$, and $Gd_{0.85}Er_{0.15}$ confirming the possibility of improving performance through layering. However, they concluded that the composition of materials in layers and their quantity should be optimized for different working conditions. Later Arnold et al. (2011) concluded from their experiments on a two-layered bed of Gd and $Gd_{0.85}Er_{0.15}$ that the highest temperature spans are achieved when the average temperature during the whole cycle in a layer is close to the Curie temperature of the layer's material. Tušek et al. (2014) experimentally tested 2-, 4-, and 7-layered parallel plate regenerators made of $LaFe_{13-x-y}Co_xSi_y$. Their experiments highlighted that for different working temperatures the optimum regenerator composition is different. Among the best performing magnetic refrigerators, the device reported by Jacobs et al. (2014) works with six layers of $LaFeSiH$. The performance of their device is also numerically simulated. Aprea et al. (2011) used two layers of equal length made of $Gd_{0.65}Tb_{0.35}$ and $Gd_{0.92}Tb_{0.08}$ in their numerical model to increase both the efficiency and cooling power compared to a single-layered regenerator. They suggest that optimum Curie temperature of each layer is equal to its average temperature.

The material for each layer should be carefully chosen to design a high performance multi-layered regenerator; however, the theoretical investigation of the problem useful at design stage has not been extensively reported in the open literature. Reid et al. (1994) suggested that the materials chosen for layers should match an adiabatic temperature change vs. temperature diagram find through thermodynamic analysis. Some other authors have highlighted the need for

the optimized selection of the materials used in regenerators (Arnold et al., 2011; Rowe and Tura, 2006). This study investigates optimizing the selection of materials, to get either high efficiency or high temperature span, which requires different selection of the materials, at design stage using a numerical simulation.

In this work measured properties of Gadolinium but with different Curie temperatures and adjusted heat capacities are used to do the theoretical optimization. Using experimentally measured material properties whose Curie temperatures are shifted or theoretical models such as mean field theory to model the layered regenerators is common; however, use of experimentally measured properties with modified heat capacity values to satisfy Maxwell equations after shifting the Curie temperatures, as done in this study, is, to the best knowledge of the authors of this article, not reported in other publications. The Curie temperatures found through the optimization can be used as a guide for the desired composition of alloys needed to have an optimized magnetic refrigerator. Reid et al. (1994) and Rowe and Barclay (2003) suggest that the magnetocaloric effect of the materials used in consecutive layers should ideally increase as the working temperature increases along the bed; nevertheless, in practice, such an increase in the magnetocaloric effect is not guaranteed when the transient temperature is tuned by changing the composition of alloys. In this study we assumed that the materials used in different layers have similar magnetocaloric effect although their Curie temperatures are different.

2 Model

The modeled system consists of a packed bed of magnetocaloric materials and a heat transfer fluid flowing through the bed. The magnetocaloric material gets warm as it is magnetized by an external magnetic field and the heat transfer fluid takes the heat from the magnetocaloric material and rejects it to the ambient in a hot heat exchanger. Demagnetizing the magnetocaloric material makes it cold, and the fluid exiting the hot heat exchanger becomes cold when it goes through the demagnetized bed. The cold heat transfer fluid absorbs heat in the cold heat exchanger and becomes warmer before entering the packed bed again. The packed bed of the magnetocaloric materials serves as both refrigerant and regenerator.

To increase the performance, the bed has 6 layers of magnetocaloric materials with similar magnetocaloric effect but different Curie temperatures. To prevent the layers from working at temperatures far from their Curie temperature, the temperature span created by the active magnetic regenerative cycles is divided equally by the number of layers. Since the temperature gradient along the bed between the cold end and the hot end is not linear, the lengths of the layers are not necessarily equal. Experimentally measured properties of Gadolinium reported by Lozano et al. (2014) are used as a basis to model materials with similar magnetocaloric effect but different Curie temperatures.

Since magnetocaloric effect, temperature, and heat capacity are interrelated through Maxwell equations (Pecharsky and Gschneidner Jr, 1999), materials with similar magnetocaloric effect

but different Curie temperatures cannot be created by merely shifting the properties along the temperature axis. In this work, to have more physically correct models of the materials with Curie temperatures other than that of Gadolinium but with similar magnetocaloric effect, the heat capacity data are modified in a way that they satisfy Maxwell's equations. For instance, Fig. 1 shows adjusted heat capacity for materials with 4 different Curie temperatures and corresponding magnetic entropy change.

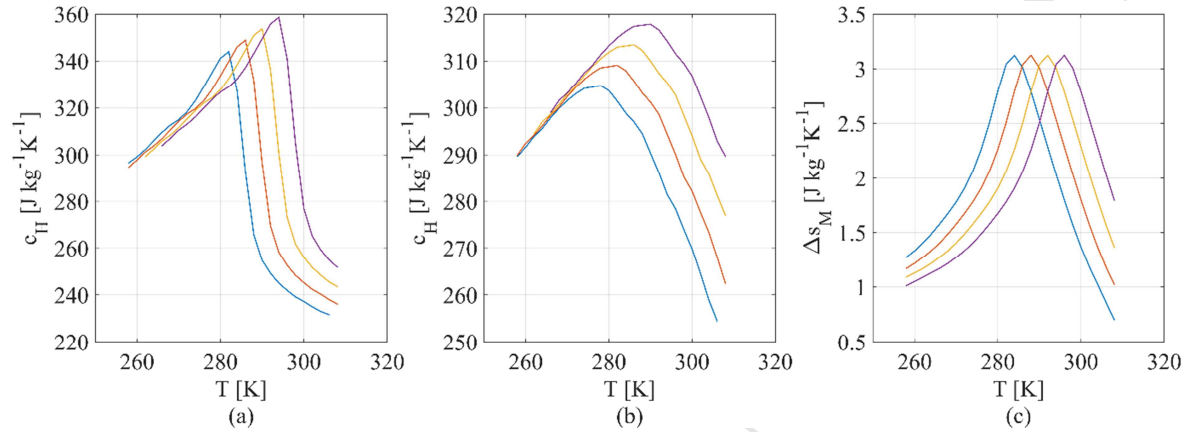


Fig. 1 (a) adjusted heat capacity at zero field, (b) adjusted heat capacity at 1T, and (c) magnetic entropy change for 0-1T field change for four materials (indicated with different colors) with different Curie temperatures

The variations in the flow of heat transfer fluid and the magnetic field, modeled based on the device described by Bjørk et al. (2010), are shown in Fig. 2a. Simpler, but less realistic for rotary devices, patterns of variation for flow rate and magnetic field, Fig. 2b, are also used to obtain the results presented in a part of section 3, Results and Discussion. Positive flow means flow from cold end to hot end and negative flow rate means flow in the opposite direction.

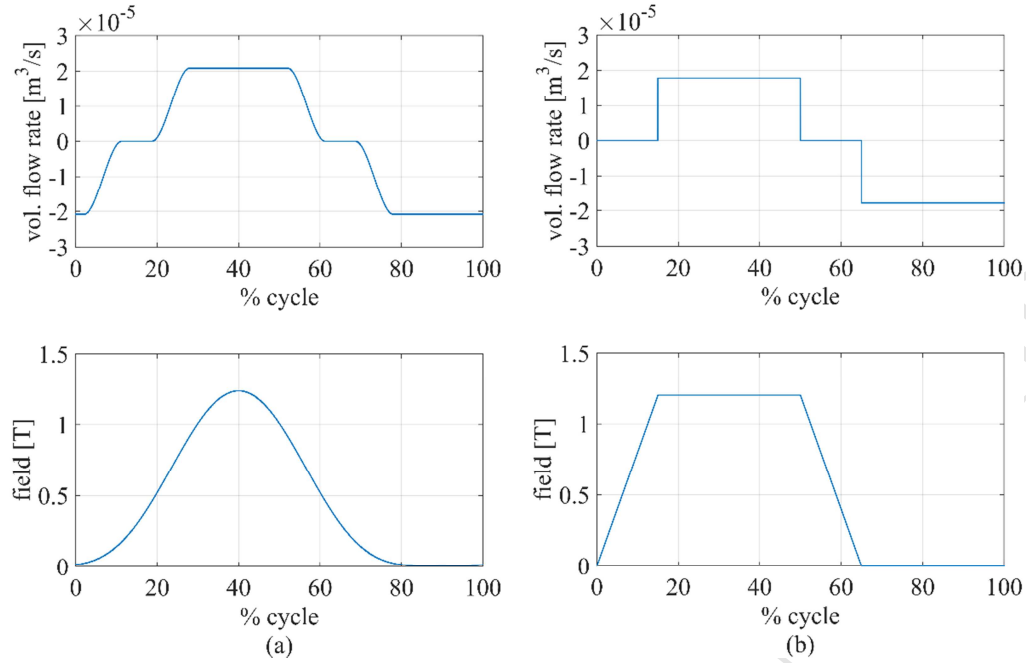


Fig. 2 (a) flow and field variations for each bed during a cycle in a rotary device (b) simpler pattern of variation for flow rate and magnetic field

By applying the first law of Thermodynamics to the solid phase of the packed bed and the heat transfer fluid going through the bed, Eq.1 and Eq. 2, which are coupled by convective heat transfer term, are derived. This is a well-established mathematical model widely used and validated by different authors (Aprea et al., 2013; Engelbrecht, 2008; Jacobs et al., 2014).

$$-(1 - \varepsilon)\rho_s T_s \frac{\partial s}{\partial B} \frac{\partial B}{\partial t} = -k_{e,s} \frac{\partial^2 T_s}{\partial x^2} - h_{sf} a (T_f - T_s) + (1 - \varepsilon)\rho_s c_{H,s} \frac{\partial T_s}{\partial t} \quad (1)$$

$$\frac{dP}{dx} V_D = \rho_f V_D c_{p,f} \frac{\partial T_f}{\partial x} - k_{e,f} \frac{\partial^2 T_f}{\partial x^2} + h_{sf} a (T_f - T_s) + \varepsilon \rho_f c_{p,f} \frac{\partial T_f}{\partial t} \quad (2)$$

The convection heat transfer coefficient, h_{sf} , is given by Eq. 3 (Kaviany, 1991; Wakao and Kaguei, 1982), which is valid for the flow through a packed bed with Re_d below 8500 (Amiri and Vafai, 1998). The effective conductivities, $k_{e,f}$ and $k_{e,s}$, are estimated by Eq. 4 and Eq. 5 (Amiri and Vafai, 1998).

$$h_{sf} = \frac{k_f}{d_p} \left(2 + 1.1 Pr^{1/3} Re_d^{0.6} \right) \quad (3)$$

$$k_{e,f} = k_f (\varepsilon + 0.5 Re_d Pr) \quad (4)$$

$$k_{e,s} = (1 - \varepsilon) k_s \quad (5)$$

The pressure drop is calculated using the modified Ergun equation, Eq. 6 (Macdonald et al., 1979).

$$-\frac{dP}{dx} = \frac{180(1-\varepsilon)^2 \mu_f}{d_p^2 \varepsilon^3} V_D + \frac{1.8 \rho_f (1-\varepsilon)}{d_p \varepsilon^3} V_D^2 \quad (6)$$

Since this study aims at optimizing the selection of magnetocaloric materials and length of layers, not predicting the absolute values of performance measures, the parts external to the packed bed such as heat exchangers, pipes, motors, etc. are excluded from the model. Demagnetization field, although not explicitly addressed in the model, is, at least to some extent, taken into account since experimentally measured magnetocaloric properties of the materials are used. Parasitic heat transfer from the ambient to the bed does not affect the suggested methods of optimization although it lowers the performance. To avoid unnecessary complications the parasitic heat transfer is excluded in the most of the study; however, to show that the parasitic heat transfer does not change the conclusions of the study, only in a small part of the results reported in section 3, Results and Discussion, it is included in the model by adding the term $\frac{4U}{D}(T_f - T_{amb})$ (with $U= 10 \text{ Wm}^{-2}\text{K}^{-1}$ and $T_{amb}= 308.15 \text{ K}$) to the right hand side of Eq. 2.

Eq. 1 and Eq. 2 are numerically solved through iteration using Backward Time, Centered Space scheme (60 spatial nodes and 8000 time steps) to find steady state solid and fluid temperatures along the bed, during a cycle. As initial condition, it is assumed that both the solid phase and the heat transfer fluid are at thermal equilibrium with heat sink. The boundary conditions are summarized in Table 1.

Table 1 Boundary conditions

Flow direction	cold end (left) to warm end (right)	hot end (right) to cold end (left)
Fluid, cold end	$T_f = T_{C,R}$	$\partial T_f / \partial x = 0$
Fluid, hot end	$\partial T_f / \partial x = 0$	$T_f = T_{H,R}$
Solid, cold/hot end	$\partial T_s / \partial x = 0$	$\partial T_s / \partial x = 0$

Carnot efficiency used in presenting the results is defined by Eq. 7.

$$\eta_{Carnot} = \frac{\left(\frac{Q_C}{Q_H - Q_C}\right)}{\left(\frac{T_{C,R}}{T_{H,R} - T_{C,R}}\right)} \quad (7)$$

In this study, cooling capacity, Q_C , is constant and heating capacity is calculated using Eq. 8.

$$Q_H = \left(\int_{V_d > 0} \dot{m}_f i_{H,L} dt - \int_{V_d < 0} \dot{m}_f i_{H,R} dt \right) / \tau \quad (8)$$

In Eq. 8, $i_{H,L}$ and $i_{H,R}$ are the enthalpies of the heat transfer fluid leaving and entering (return from the hot heat exchanger) the hot end of the regenerator, respectively.

The enthalpy of the heat transfer fluid entering the cold end of the regenerator, $i_{C,R}$, is calculated using Eq. 9. The temperature corresponding to this enthalpy, $T_{C,R}$, is used to calculate the temperature span defined as $T_{H,R}-T_{C,R}$.

$$i_{C,R} = \frac{\int_{V_d < 0} \dot{m}_f i_{C,L} dt + Q_C \tau}{\int_{V_d > 0} \dot{m}_f dt} \quad (9)$$

3 Results and Discussion

The reported results are obtained with fixed hot side return temperature of 308.15 K (35 °C), flow and field variations as shown in Fig. 2a or Fig. 2b, cycle duration of 1.5 s, and cooling load of 8.4 W. Cross section area and length of the packed bed are $2.325 \times 10^{-4} \text{ m}^2$ and 0.1 m. The particles in the bed are spheres of $6 \times 10^{-4} \text{ m}$ diameter leaving void fraction of 0.36 for the heat transfer fluid to flow in between. The heat transfer fluid is ethylene glycol with 20% volume concentration. The temperature span and Carnot efficiency curves shown in the figures are made by spline curve fitting through 100 calculated points.

As the first step, the Curie temperature of each layer was chosen as the temperature of the magnetocaloric material in the layer averaged over both space and time during a cycle. For a six-layered bed, as described in section 2, with Curie temperatures equal to the average temperature of each layer of magnetocaloric materials during one cycle and field and flow variations given by Fig. 2a, the average temperature along the bed varies as shown in Fig. 3. The obtained temperature span and Carnot efficiency with this approach are 36.4 K and 18.1 %.

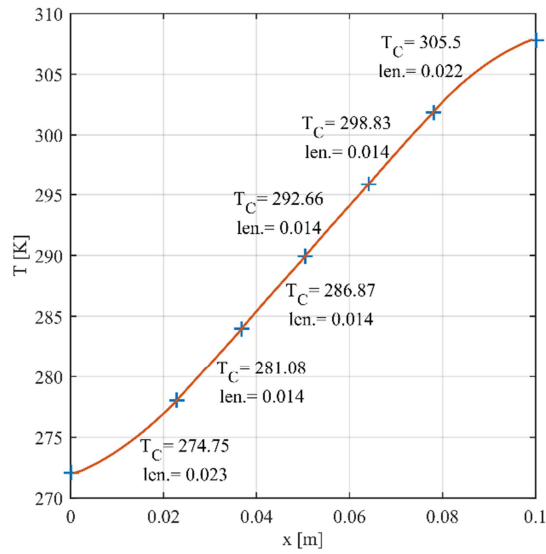


Fig. 3 Average temperatures during a cycle at each point along the bed, when Curie temperatures are chosen as average temperatures of layers during the whole cycle with field and flow variations indicated in Fig. 2a. Curie temperature and length [m] of each layer is written on it. Borders of the layers are indicated by “+”.

The temperature along the bed, as shown in Fig. 4, varies during a cycle following the changes in magnetic field and flow of heat transfer fluid. Such variations in the temperature suggest that different results can be obtained if choosing of the Curie temperatures is done based on the bed temperatures at different moments during a cycle instead of the whole cycle average. Fig. 5 shows how the temperature span and Carnot efficiency vary as different moments of a cycle are used to indicate the spatial average layer temperatures, chosen as Curie temperatures. The Curie temperatures resulting in the highest temperature span and the highest Carnot efficiency are shown in Fig. 6 and Fig. 7. Similarities between Fig. 3 and Fig. 6 reveal why the temperature span calculated by the Curie temperatures equal to the average temperature of layers during whole cycle, 36.4 K, is so close to the maximum temperature span in Fig. 5, 36.6 K.

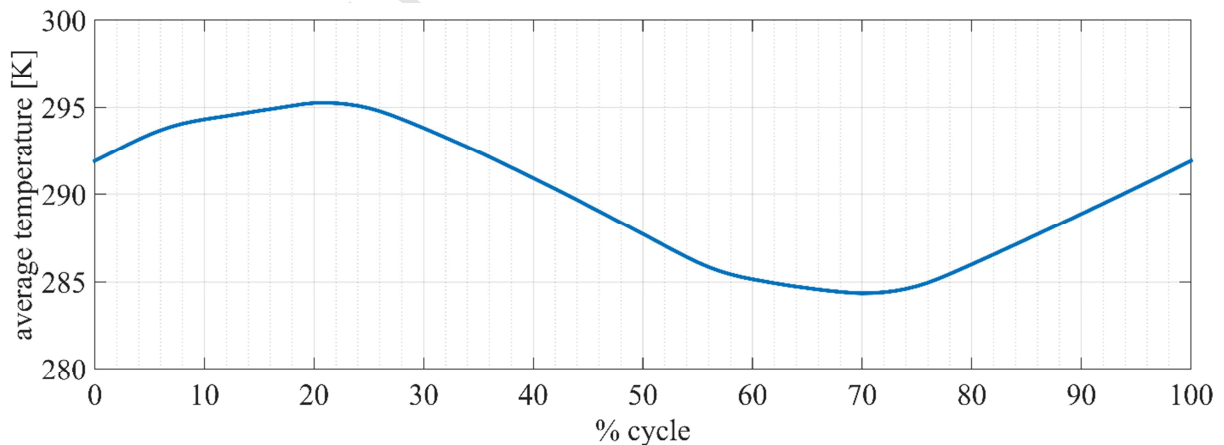


Fig. 4 average temperature of the bed with Curie temperatures selected as shown in Fig. 3 during a cycle

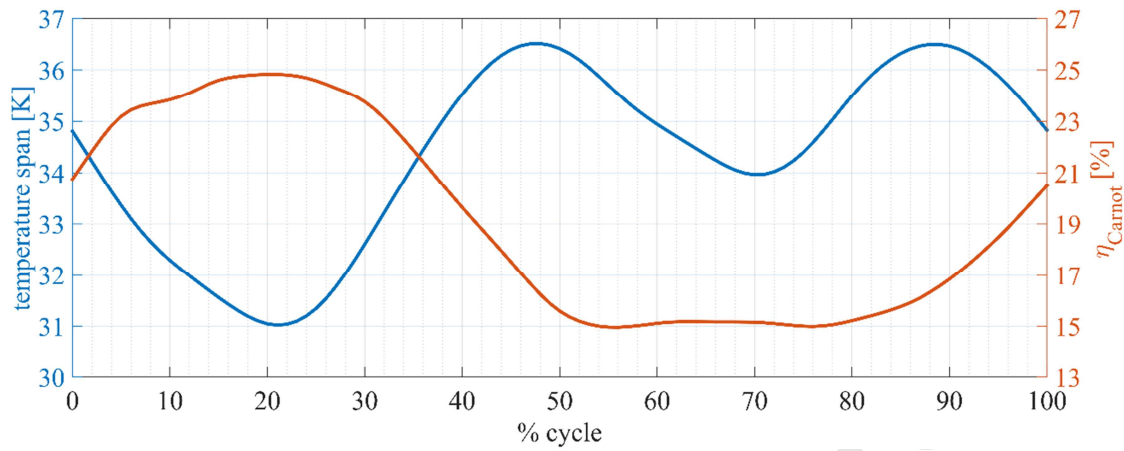


Fig. 5 temperature span created between the two ends of the regenerator and Carnot efficiency for Curie temperatures chosen to match the bed temperature at different moments during a cycle with field and flow variations indicated in Fig. 2a. The horizontal axis shows the moment at which spatial average layer temperatures, used as Curie temperatures, are calculated.

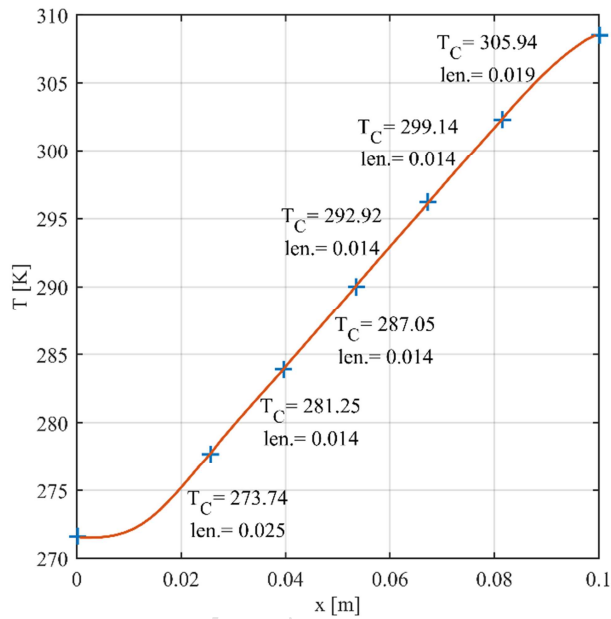


Fig. 6 temperature of solid along the bed at the moment 0.47τ of a cycle with field and flow variations indicated in Fig. 2a. Curie temperatures, given for each layer, are chosen based on the temperatures at this moment. Borders of layers are indicated by "+". These Curie temperatures give the highest temperature span in Fig. 5.

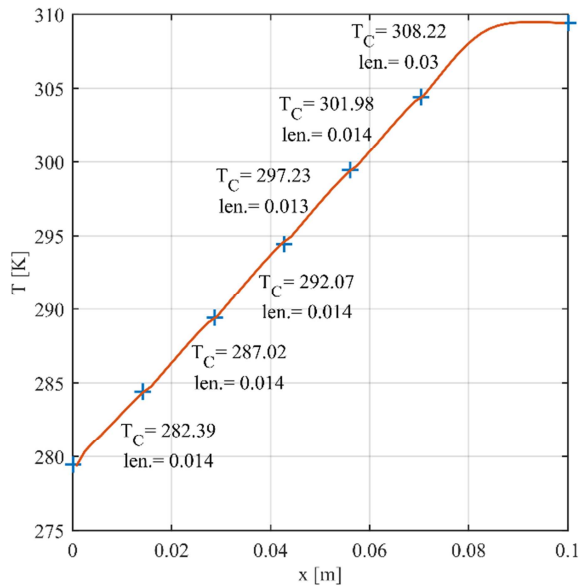


Fig. 7 temperature of solid along the bed at the moment 0.21τ of a cycle with field and flow variations indicated in Fig. 2a. Curie temperatures, given for each layer, are chosen based on the temperature at this moment. Borders of layers are indicated by “+”. These Curie temperatures give the highest Carnot efficiency in Fig. 5.

Fig. 5 suggests that optimizing for large temperature span and for high Carnot efficiency need different layer designs since the maximum efficiency is accompanied by a relatively low temperature span and vice versa. By plotting Carnot efficiencies versus temperature spans, Fig. 8, it can be observed that the Carnot efficiency decreases with the increase of temperature span. The increased axial diffusion when the temperature span is large leads to lower efficiency of the cycle (Bejan, 1989). Such an increase is due to the increased temperature gradient, not the insignificant change in the thermal conductivity of the materials. In addition, the higher viscous dissipation and pumping power, due to the increased viscosity of the heat transfer fluid at the lower temperatures reached with larger spans and fixed heat sink temperature, make the refrigerator less efficient.

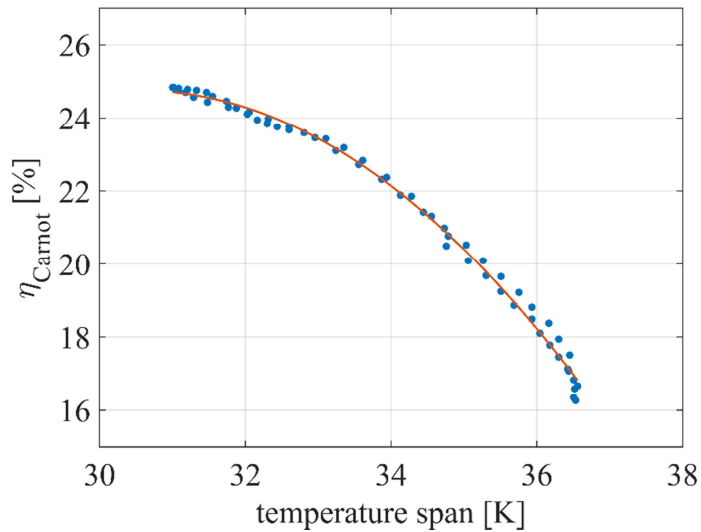


Fig. 8 Carnot efficiencies vs temperature spans shown in Fig. 5 (except for the section between the two peaks of temperature span) and a quadratic polynomial fitted curve as a guide to the eye

Considering Fig. 4 together with Fig. 5, it can be seen that the maximum temperature span, 36.6 K, is calculated when the temperature of the bed is close to the average temperature of the whole cycle, 289.8 K, while the maximum Carnot efficiency, 24.8 %, is calculated at the maximum average temperature.

As Fig. 1c shows, the magnetocaloric effect is rather symmetrical about the Curie temperature. Therefore, choosing Curie temperature of each layer equal to the average temperature of the layer during the cycle maximizes the magnetocaloric effect. As the results indicate, the maximized magnetocaloric effect in the layers results in the highest temperature span achieved by layering, which is in accordance with the conclusions that Arnold et al. (2011) have made from their experimental work.

Different factors are involved in determining the Carnot efficiency values shown in Fig. 5. With small temperature spans, as discussed above, the axial diffusion and viscous dissipation losses are smaller; therefore, using the warmest moment of the cycle to choose the Curie temperatures of the layers, by which the temperature span is minimum, tend to result in higher Carnot efficiencies. In addition, when the Curie temperatures of the layers are chosen in a way that they are above the average temperature of the layers during the cycle, most of the magnetocaloric materials are at temperatures below the Curie temperature during a cycle. Such choice of Curie temperatures results in gradual increase in magnetocaloric effect in each layer from its colder end to the warmer end, which is in line with the increase of magnetocaloric effect from colder to warmer temperatures suggested by Reid et al. (1994). On the other hand, choosing the Curie temperatures too far from the average working temperatures of the layers results in too small magnetocaloric effect relative to the losses; therefore, it adversely affects the Carnot efficiency. In all of the conditions tested in this study, choosing the Curie temperatures based on the

warmest moment of the cycle lead to high Carnot efficiency. However, to get the absolute maximum Carnot efficiency, considering the multiplicity of the relevant factors, Curie temperatures few Kelvins higher and lower should be tried.

With flow rate and magnetic field patterns of variation shown in Fig. 2a, the maximum Carnot efficiency is obtained when the Curie temperatures are chosen as spatial average layer temperature plus 1.2 K (Fig. 9a). As shown in Fig. 9a, by adding 2 to 6 K to the average layer temperature as Curie temperature, the peak Carnot efficiency achieved by using temperatures of the moment 0.21τ , the warmest moment of the cycle, goes down and two peaks around it appear, which shows that the average temperature at moment 0.21τ plus 2 K and above as Curie temperatures are too far from the working temperatures of layers (resulting in too low magnetocaloric effect) to give high Carnot efficiency. With flow rate and magnetic field patterns of variation shown in Fig. 2b, Curie temperatures equal to 0.5 K higher than the spatial average layer temperatures at the warmest moment of the cycle, which is the last moment of magnetization process, give the maximum Carnot efficiency (Fig. 10a). In brief, using the warmest moment of the cycle, and also trying temperatures higher than the average temperatures at the warmest moment can lead to a layer design with high Carnot efficiency.

On the other hand, the valleys between the two temperature span peaks in Fig. 9b and Fig. 10b become shallower by choosing the spatial average temperature at each moment plus few Kelvins as Curie temperature. It indicates that the reduced temperature span between the two peaks in Fig. 5 is because of too low Curie temperatures. When the Curie temperatures are far from the average temperature of the cycle the magnetocaloric effect is not maximum anymore. That the peak temperature spans in the Fig. 9b are not higher or lower than the peaks in Fig. 5, but shifted horizontally confirms that the average temperatures of the layers during the whole cycle are optimum Curie temperatures to get large temperature span.

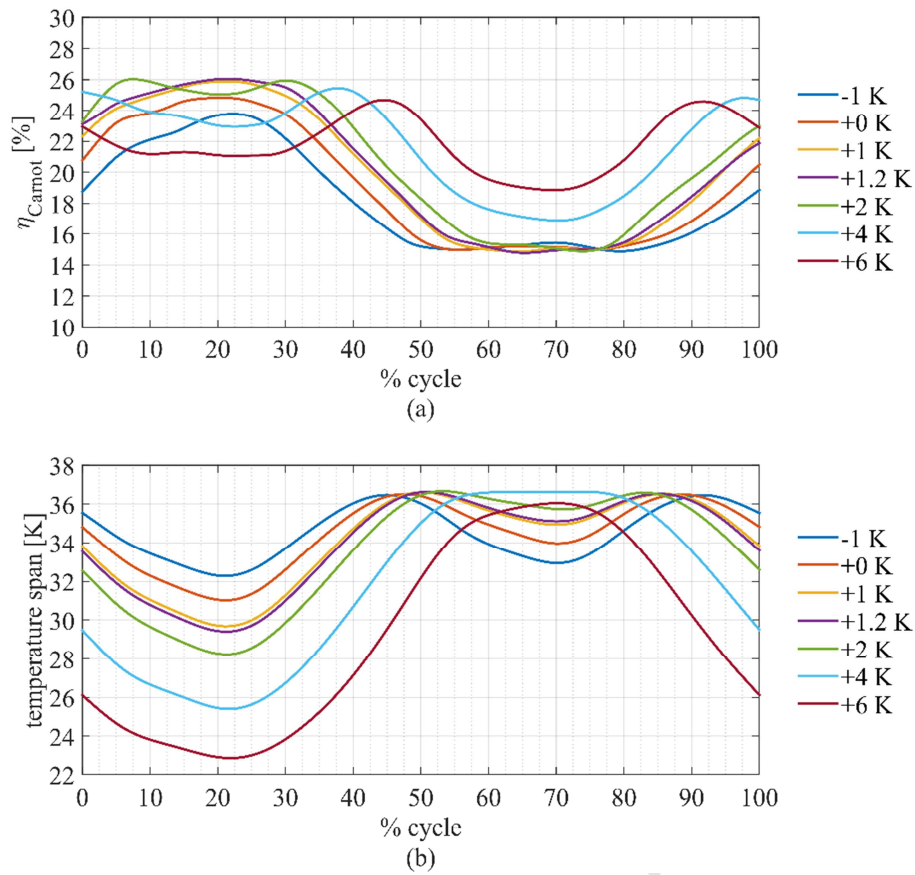


Fig. 9 The horizontal axes show the moments at which the spatial average layer temperatures, used as Curie temperatures, are calculated. Flow rate and magnetic field vary as shown in Fig. 2a. a) Carnot efficiency for Curie temperatures chosen as the average temperatures at different moments during a cycle plus -1 to 6 K b) Temperature span for Curie temperatures chosen as the average temperatures at different moments during a cycle plus -1 to 6 K

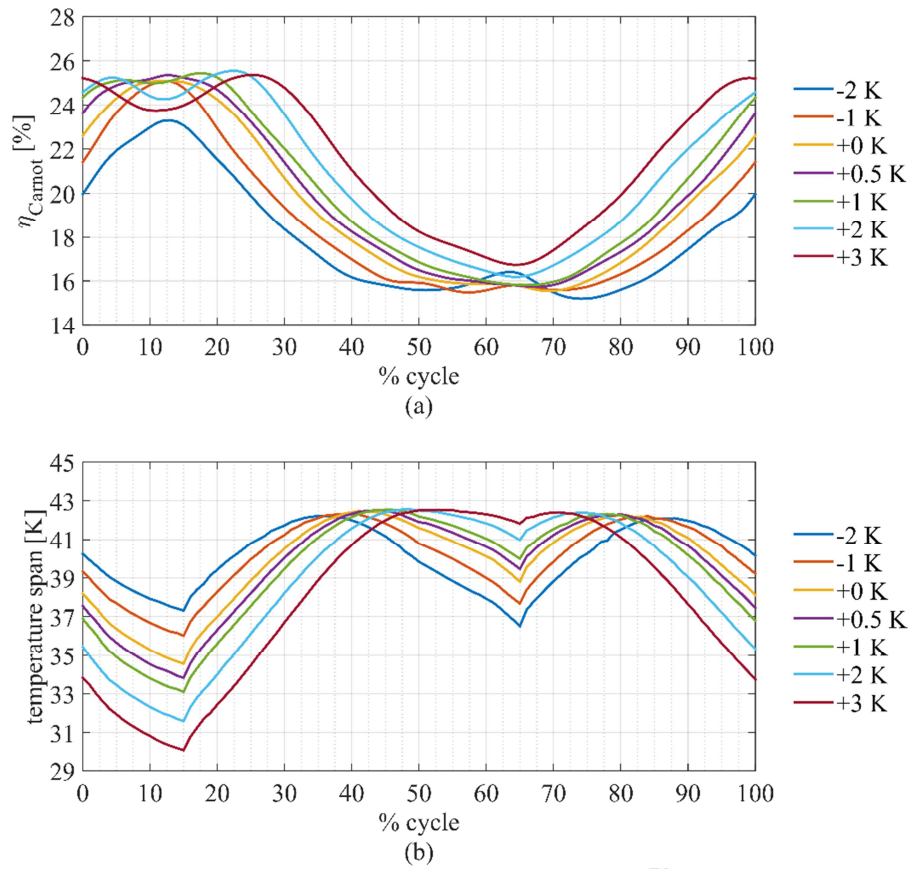


Fig. 10 The horizontal axes show the moments at which the spatial average layer temperatures, used as Curie temperatures, are calculated. Flow rate and magnetic field vary as shown in Fig. 2b. a) Carnot efficiency for Curie temperatures chosen as the average temperatures at different moments during a cycle plus -2 to 3 K b) Temperature span for Curie temperatures chosen as the average temperatures at different moments during a cycle plus -2 to 3 K

Although parasitic heat transfer from ambient to the bed can reduce the performance significantly, still the highest temperature span is achieved with Curie temperatures maximizing the magnetocaloric effect and the highest Carnot efficiency is achieved when the temperatures at the warmest moment or even a few Kelvins above are used for Curie temperatures of the layers (see Fig. 11). In other words, parasitic heat transfer from the ambient mainly shifts the plots down.

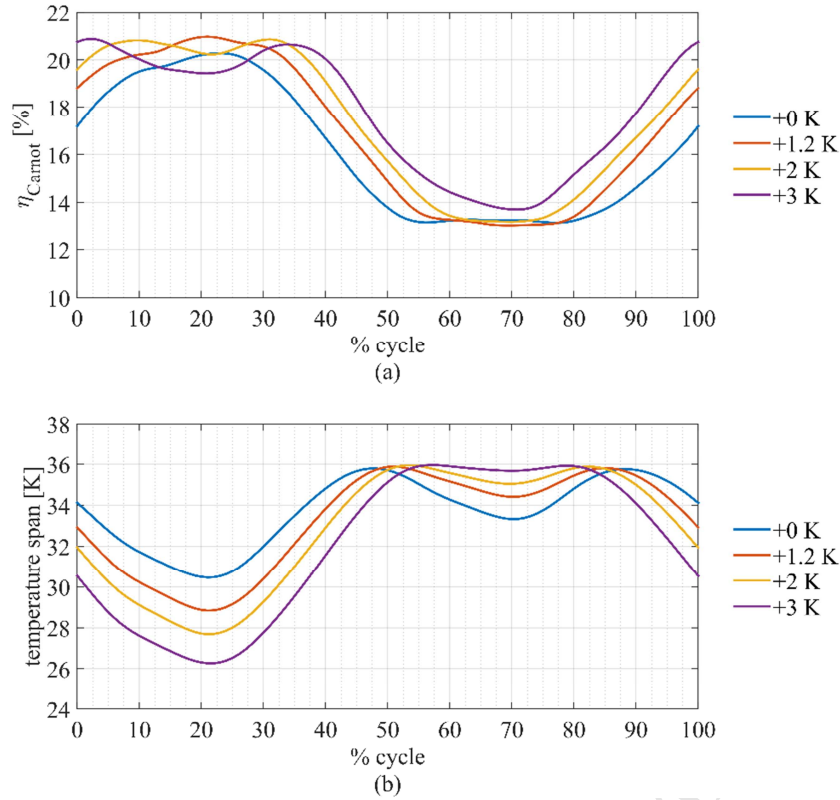


Fig. 11 The horizontal axes show the moments at which the spatial average layer temperatures, used as Curie temperatures, are calculated. Parasitic heat transfer from ambient to the bed is considered as explained in section 2. Flow rate and magnetic field vary as shown in Fig. 2a a) Carnot efficiency for Curie temperatures chosen as the average temperatures at different moments during a cycle plus 0 to 3 K b) Temperature span for Curie temperatures chosen as the average temperatures at different moments during a cycle plus 0 to 3 K

4 Conclusions

To optimize regenerators of a magnetic refrigerator for large temperature span or high efficiency, two approaches for selection of materials of the packed beds are suggested. The optimization is done using a numerical model developed to simulate the magnetocaloric effect and regeneration in a multi-layered packed bed of magnetocaloric materials. Lengths of the layers are determined by the simulation program to divide the total temperature span equally between the layers. The simulation results for a fixed heat sink temperature of 308.15 K and cooling load of 8.4 W for various magnetocaloric material selections and two different sets of patterns for variations in flow rate and magnetic field are reported.

This study shows that the layer design to get maximum temperature span is different from the layer design for maximizing Carnot efficiency. In fact, higher values of one of them lead to lower values of the other one (Fig. 8). Maximum temperature span can be achieved by choosing the materials which have the highest magnetocaloric effect in the working temperature range, while the highest Carnot efficiencies are achieved by choosing materials with Curie temperatures above the average layer temperature during a cycle. In this study, the maximum Carnot

efficiency is achieved with Curie temperatures 1.2 K above the spatial average layer temperature at the warmest moment of cycle with field and flow variations shown in Fig. 2a. For the other field and flow rate variations shown in Fig. 2b, the maximum Carnot efficiency is calculated with Curie temperatures equal to the spatial average of the temperatures of the layers at the warmest moment of cycle plus 0.5 K. In brief, using the warmest moment of the cycle, and also trying temperatures higher than the average temperatures at the warmest moment can lead to a layer design with high Carnot efficiency. In addition, the study shows that the temperature span and efficiency of a magnetic refrigerator with a fix cooling load are highly sensitive to the working temperatures.

The Curie temperatures giving the highest temperature span or Carnot efficiency obtained from a similar study can be a guide for choosing materials with certain compositions for different layers in an actual machine. Provided that the experimentally measured properties of the materials in different layers are available to the simulation software, the optimization results will be more accurate.

Further investigations using other families of materials can show whether the optimization approaches proposed in this study can be generalized for all materials.

5 Acknowledgements

The authors would gratefully like to acknowledge that this study was financed by the Swedish Energy Agency, grant number 33847-1, and Electrolux through the research program EFFSYS+.

6 References

- Amiri, A., Vafai, K., 1998. Transient analysis of incompressible flow through a packed bed. *Int. J. Heat Mass Transf.*, 41, 4259-4279.
- Aprea, C., Greco, A., Maiorino, A., 2011. A numerical analysis of an active magnetic regenerative cascade system. *Int. J. Energy Res.*, 35, 177-188.
- Aprea, C., Greco, A., Maiorino, A., 2013. A dimensionless numerical analysis for the optimization of an active magnetic regenerative refrigerant cycle. *Int. J. Energy Res.*, 37(12), 1475-1487.
- Arnold, D.S., Tura, A., Rowe, A., 2011. Experimental analysis of a two-material active magnetic regenerator. *Int. J. Refrigeration*, 34, 178-191.
- Bejan, A., 1989. Theory of heat transfer-irreversible refrigeration plants. *Int. J. Heat Mass Transf.*, 32, 1631-1639.
- Bjørk, R., Bahl, C. R. H., Smith, A., Christensen, D. V., and Pryds, N., 2010. An optimized magnet for magnetic refrigeration. *J. Magn. Magn. Mater.*, 322, 3324-3328.

- Cam Thanh, D.T., Brück, E., Tegus, O., Klaasse, J.C.P., Buschow, K.H.J., 2007. Influence of Si and Ge on the magnetic phase transition and magnetocaloric properties of MnFe(P,Si,Ge). *J. Magn. Magn. Mater.*, 310, e1012-e1014.
- Canepa, F., Cirafici, S., Napolitano, M., Merlo, F., 2002. Magnetocaloric properties of Gd₇Pd₃ and related intermetallic compounds. *IEEE Trans. Magn.*, 38, 3249-3251.
- Dai, W., Shen, B.G., Li, D.X., Gao, Z.X., 2000. New magnetic refrigeration materials for temperature range from 165 K to 235 K. *J. Alloys Compd.*, 311, 22-25.
- Engelbrecht, K., 2008. A Numerical Model of an Active Magnetic Regenerator Refrigerator with Experimental Validation. PhD, University of Wisconsin-Madison.
- Jacobs, S., Auringer, J., Boeder, A., Chell, J., Komorowski, L., Leonard, J., Russek, S., Zimm, C., 2014. The performance of a large-scale rotary magnetic refrigerator. *Int. J. Refrigeration*, 37, 84-91.
- Kaviany, M., 1991. Principles of Heat Transfer in Porous Media, Springer-Verlag.
- Lozano, J.A., Engelbrecht, K., Bahl, C.R.H., Nielsen, K.K., Barbosa JR, J.R., Prata, A.T., Pryds, N., 2014. Experimental and numerical results of a high frequency rotating active magnetic refrigerator. *Int. J. Refrigeration*, 37, 92-98.
- Macdonald, I.F., El-Sayed, M.S., Mow, K., Dullien, F.A.L., 1979. Flow through Porous Media—the Ergun Equation Revisited. *Ind. Eng. Chem. Funda.*, 18, 199-208.
- Monfared, B., Furberg, R., Palm, B., 2014. Magnetic vs. vapor-compression household refrigerators: A preliminary comparative life cycle assessment. *Int. J. Refrigeration*, 42, 69-76.
- Pecharsky, A.O., Gschneidner Jr., K.A., Pecharsky, V.K., Schindler, C.E., 2002. The room temperature metastable/stable phase relationships in the pseudo-binary Gd₅Si₄–Gd₅Ge₄ system. *J. Alloys Compd.*, 338, 126-135.
- Pecharsky, V.K., Gschneidner Jr., K.A., 1999. Magnetocaloric effect and magnetic refrigeration. *J. Magn. Magn. Mater.*, 200, 44-56.
- Reid, C.E., Barclay, J.A., Hall, J.L., Sarangi, S., 1994. Selection of magnetic materials for an active magnetic regenerative refrigerator. *J. Alloys Compd.*, 207-208, 366-371.
- Richacrd, M.A., Rowe, A.M., Chahine, R., 2004. Magnetic refrigeration: Single and multimaterial active magnetic regenerator experiments. *J. Appl. Phys.*, 95, 2146-2150.
- Rowe, A., Tura, A., 2006. Experimental investigation of a three-material layered active magnetic regenerator. *Int. J. Refrigeration*, 29, 1286-1293.

Rowe, A.M., Barclay, J.A., 2003. Ideal magnetocaloric effect for active magnetic regenerators. *J. Appl. Phys.*, 93, 1672-1676.

Tušek, J., Kitanovski, A., Tomc, U., Favero, C., Poredoš, A., 2014. Experimental comparison of multi-layered La-Fe-Co-Si and single-layered Gd active magnetic regenerators for use in a room-temperature magnetic refrigerator. *Int. J. Refrigeration*, 37, 117-126.

Wakao, N., Kaguei, S., 1982. *Heat and Mass Transfer in Packed Beds*, New York, Gordon and Breach, Science Publishers, Inc.

- Optimized design of regenerator of magnetic refrigerator is investigated
- Optimal temperature span and efficiency need different regenerator designs
- Layer average temperature as material's Curie temperature maximizes span
- Curie temperature above layer's average temperature maximizes efficiency
- Temperature span and efficiency are highly sensitive to the working temperatures

ACCEPTED MANUSCRIPT